Airway Remodeling in Ferrets with Cigarette Smoke Induced COPD using µCT Imaging

Denise Stanford,[1,2] Harrison Kim,[4] Sandeep Bodduluri,[2,3] Jennifer LaFontaine,[1,2] Stephen A. Byzek,[1,2] Trenton R. Schoeb,[6] Elex S. Harris,[1,2] Hrudaya P. Nath,[3,4] Surya P. Bhatt,[2,3] S. Vamsee Raju,[1,2] and Steven M. Rowe,[1,2,5]

[1]Cystic Fibrosis Research Center, [2]Department of Medicine, [3]UAB Lung Imaging Core, [4]Department of Radiology, [5]Departments of Pediatrics and Department of Cell Developmental and Integrative Biology, [6]Genetics and Animal Resources Program, all at the University of Alabama at Birmingham, Birmingham, AL USA

Corresponding author: Steven M. Rowe, M.D., University of Alabama at Birmingham, Cystic Fibrosis Research Center, Department of Medicine, Division of Pulmonary, Allergy and Critical Care Medicine, MCLM 702, 1918 University Blvd, Birmingham, AL 35294. Email: smrowe@uab.edu Phone: (205) 934-9640 Fax: (205) 934-7315

Funding Source: NIH grants R35HL135816 (to SMR) and P30 DK072482 (to SMR) and K23HL133438 (to SPB) and 1R01AA027528 (to SVR)

Running Head: Airway Remodeling in Ferrets with COPD

Author Contributions:
Study concept and design: DS, HK, HPB, SVR, SMR
Conducted experiments: DS, SAB, JL
Interpreted results: DS, HK, ESH, SMR
Prepared Figures: DS, HK, ESH, TRS, SMR
Drafting of the manuscript: DS, SB, HK, SMR
Supervised the project: SVR, SMR
All authors provided critical review and approved the manuscript for submission.

Manuscript Word Count: 5352
Method Word Count: 1637 **Note:** An aspect of this manuscript is a novel method, hence we have eclipsed the 500 word limit. This section can be shortened with use of a supplement if desired by the editor.

This manuscript includes an online data supplement that is presently on a secure server for peer review: http://doi.org/10.5281/zenodo.3751865

Abstract

RATIONALE: Structural changes to airway morphology such as increased bronchial wall thickness (BWT) and airway wall area are cardinal features of chronic obstructive pulmonary disease (COPD). Ferrets are a recently established animal model uniquely exhibiting similar clinical and pathological characteristics of COPD as humans, including chronic bronchitis.

OBJECTIVES: Develop a μCT method for evaluating structural changes to the airways in ferrets, and assess whether the effects of smoking induce changes consistent with chronic bronchitis in humans.

METHODS: Ferrets were exposed to mainstream cigarette smoke or air control twice daily for 6 months. μCT was conducted in vivo at 6 months; a longitudinal cohort was imaged monthly. Manual measurements of BWT, luminal diameter (LD), and BWT:LD ratio were conducted, and confirmed by a semi-automated algorithm. The square root of bronchial wall area ($\sqrt{WA}$) vs. luminal perimeter was determined on an individual ferret basis.

MEASUREMENTS AND MAIN RESULTS: Smoke exposed ferrets reproducibly demonstrated 34% increased BWT ($P<0.001$); along with increased LD, and BWT:LD ratio vs. air controls. Regression indicated the effect of smoking on BWT persisted despite controlling for covariates. Semi-automated measurements replicated findings. $\sqrt{WA}$ for the theoretical median airway luminal perimeter of 4 mm (Pi4) was elevated 4.4% in smoke exposed ferrets ($P=0.015$). Increased BWT and Pi4 developed steadily over time.

CONCLUSIONS: μCT-based airway measurements in ferrets are feasible and reproducible. Smoke exposed ferrets develop increased BWT and Pi4, changes similar to humans with chronic bronchitis. μCT can be used as a significant translational platform to measure dynamic airway morphological changes.

Abstract Word Count: 250/250

Keywords: COPD, chronic bronchitis, bronchial wall thickness
Descriptor number: 9.4 COPD: Comorbidities

Funding: NIH grants R35HL135816 (to S.M.R.) and P30 DK072482 (to S.M.R.)

Introduction

Chronic obstructive pulmonary disease (COPD) is characterized by progressive airflow obstruction and is currently the third leading cause of death in the United States (25). COPD, most frequently caused by cigarette smoking, results in emphysema that principally features destruction of lung parenchyma; chronic bronchitis, characterized by chronic mucus hypersecretion and expectoration (9, 25); or often a mix of these phenotypes. The protean effects of emphysema and chronic bronchitis that vary in severity on an individual basis makes it challenging to sub-phenotype and monitor COPD, thus limiting the ability to characterize relevant mechanisms, the severity of disease expression and progression, and response to targeted treatment (8). This is particularly important for the diagnosis of chronic bronchitis, which afflicts approximately 60% of individuals with COPD, and in which specific therapies are only beginning to emerge.

Computed tomography (CT) is increasingly being used to visualize structural changes associated with emphysema (parenchymal destruction) and airway remodeling (bronchial wall thickening, airway narrowing, or even loss of small airways in its extreme form) (2). Recent advances in CT image-processing techniques have led to accurate segmentation of airways and lung structures in patients, thus enabling the characterization of COPD population into emphysema and chronic bronchitis predominant sub-groups. Chronic bronchitis associated airway remodeling in COPD has been successfully quantified by estimating bronchial diameters and airway wall thickness on CT images acquired at full inspiration (10, 15). Pi10 measurements, where multiple measurements of the relationship between airway perimeter and

bronchial wall area are determined on an individual basis, and then calculated for a theoretical airway with a luminal circumference of 10 mm (approximating a segmental airway), were devised to avoid bias due to between-subject differences in airway sizes. Using this calculation, Pi10 increases with worsening chronic bronchitis and airway disease, and can be used as an effective outcome measure (7, 12, 14, 19). These techniques have improved our understanding of COPD progression in patients, but have not yet been coupled to experimental models with prominent airway disease to reveal novel pathophysiological targets.

Animal models that recapitulate the morphological changes to the airways and exhibits spontaneous lung disease due to cigarette smoking are needed to accelerate our mechanistic understanding and help evaluate novel therapeutic targets of COPD-related airway disease (4). While mice have been a powerful model, particularly for lung matrix destruction that accompanies emphysema and the genetic contribution to these pathways, they do not exhibit many of the mucosal abnormalities present in ferrets, including clinical and mechanistic features of chronic bronchitis (5). Previously, we have demonstrated that ferrets chronically exposed to cigarette smoke exhibit similar clinical and pathological features associated with COPD in humans (20). With smoke exposure, ferrets develop chronic bronchitis, including the presence of chronic cough, histologic evidence of chronic mucus hypersecretion, and glandular hyperplasia, in addition to emphysematous lung parenchyma. To fully exploit the model, novel biomarkers of pathophysiology and clinical response are needed.

We hypothesized that μCT imaging of the ferret model of COPD could enable non-invasive demonstration of key features of airway remodeling, including increased

bronchial wall thickness that progresses longitudinally, providing a crucial, non-invasive, and potentially responsive serial biomarker with direct clinical relevance. In this manuscript, we establish increased bronchial wall thickness and elevated bronchial wall area in smoke exposed ferrets that is dynamic, providing a longitudinal outcome measure well-suited for the evaluation of novel therapies.

Methods

Ferret model of COPD

All animal protocols were reviewed and approved by the University of Alabama at Birmingham Institutional Animal Care and Use Committee (IACUC). Age and sex matched wild type ferrets (*Mustela putorius furo*) were exposed to diluted mainstream cigarette smoke following age of maturity (17-20 weeks of age) from 3R4F research cigarettes (Univ. of Kentucky, Lexington, KY) using an automated cigarette smoking apparatus (TSE Systems, Chesterfield, MO). Ferrets were exposed to 200 µg/l of total particulate matter, 35-ml puffs of 2-s duration at a rate of 3 L/sec as previously described (20). All ferrets were imaged by µCT at 6 months of cigarette smoke exposure. A sub-cohort underwent µCT at baseline and monthly thereafter through six months. Ferret weights by sex were recorded after 6 months of smoke exposure; smokers showed no statistical difference when compared to controls (23 smoke, 14 control) (Supplemental Table 1).

µCT imaging

We conducted non-contrast CT imaging of ferrets under inhaled isoflurane anesthesia and prospectively gated for a single inspiratory phase of respiration using a µCT scanner (MiLabs, Utrecht, Netherlands) (Supplemental Figure 1). All images were acquired at ultra-focused magnification with respiratory gating and the following parameters: tube voltage (55 kV), tube current (0.19 mA), scan angle (360^{o}), and 20 ms of exposure. All images were reconstructed using vendor software at 40 µm/voxel resolution for manual measurements and 80 µm/voxel for semi-automated

measurements at a single respiratory phase; reconstruction at lower voxel counts did not impact resolution due to limitations in respiratory gating of spontaneously breathing animals. Post-reconstruction, images were filtered using 0.5 mm Gaussian smoothing kernel on PMOD software (PMOD Technologies LLC, Zurich, Switzerland).

Manual measurements of airway morphology

The segmental and sub-segmental bronchial wall thickness is commonly measured to assess degree of airway remodeling in COPD patients (2). To conduct this in ferrets, airways were selected based on the ability to routinely visualize them by μCT and produce the measurements at specific anatomic locations in a reproducible fashion between ferrets. Lungs were divided into apical, medial and caudal sections and a single 5^{th} (or 6^{th} when the 5^{th} was not well visualized) generation airway from each region were measured for both the left and right lung. Typical 5^{th} to 6^{th} generation airways, using the sum of airway wall plus lumen, are estimated between 1.4 to 1.6 mm in males, which is approximately 50% of the size of the corresponding airway in humans, but with otherwise similar histological structure; noting length is 25-50% smaller in females, and airway lumen ~50% of the total airway diameter, this corresponds to luminal airway measurements between 0.4 to 0.8 mm in females (17). The analyst was blinded to exposure type. For each selected airway, the axial image view was used for bronchial wall thickness (BWT) and luminal diameter (LD) measurements at the midpoint of each segment, confirmed by segmental image view so as to avoid the impact of airway branching, and BWT/LD ratio calculated (Figure 1A). This resulted in six airway measurements for each animal (N= 23 smoke, 19 control for

left and right apical, medial, and caudal lobes, respectively). We compared the mean values of these six airway measurements between smoke exposed ferrets and controls, both with each airway treated as an individual variable and averaged as a single point estimate of these parameters for each ferret. A second analyst, also blinded to treatment assignment, recapitulated measurements from a subset of ten ferrets (N= 5 smoke, 5 control). The airway perimeter was calculated by LD*π and the square root of the wall area by $\sqrt{(\pi * (BWT^2 + LD * BWT)}$. A regression line was then generated between airway perimeter and $\sqrt{WA}$ for each ferret. Since the average mean internal luminal perimeter in control ferrets was ~2 mm for the manual method, we estimated the $\sqrt{WA}$ of airways with internal perimeters of 2 mm, termed Pi2.

Semi-automated measurement of bronchial wall thickness

We authored a customized semi-automated version to recapitulate the measurement of ferret bronchial wall thickness, but limited this to the apical lobe due to reproducibility of the procedure. First, the entire region of the airway lumen was segmented using a region-growing method (22), when the seed pixel was selected at the center of the cranial trachea (threshold: ≤ -900 HU) to initiate airway mapping (Supplemental Figure 2A). Then the 4^{tjh} to 6th generation of apical lobe airway in both the left and right lungs were selected for analysis (Supplemental Figure 2B), noting this is more proximal than could be reliably achieved with manual measurements enabled by the region growing method. The 3-dimensional CT image was vertically re-oriented for each airway generation so that it was vertical to the image slices. Vertical re-orientation was a 3D rotation of the image so the selected airway was vertical to the

196 axial image slices, facilitating sequential axial cuts to determine bronchial wall area.
197 Vertical re-orientation was implemented in the following steps. First, the centroid of the
198 airway lumen was determined in each image slice. Second, a line fitting the centroids of
199 the image slices was determined, and the angle between the fitted line and the vertical
200 axis calculated (Supplemental Figure 2C). Third, the 3D image was rotated to align with
201 the vertical axis (Supplemental Figure 2D).

202 In each image slice, the binary luminal region was obtained using a region-
203 growing method after the seed pixel was selected at the center of trachea (threshold: ≤ -
204 900HU) and dilated twelve times sequentially (40-μm increase at each dilation) (1),
205 creating an iso-distance shell region (40-μm thickness) at each iteration by $SR_n = DLR_n$
206 $– DLR_{n-1}$, where SR_n and DLR_n are the shell region and the dilated luminal region,
207 respectively, at the n^{th} iteration (Supplemental Figures 3A and 3B). The pixel values of
208 the bronchial wall on each shell region were averaged, and the bronchial wall thickness
209 (BWT) was determined as twice the distance from the original luminal boundary to the
210 shell region having the maximum mean pixel value (Supplemental Figure 3C). The
211 luminal diameter (LD) and perimeter were calculated by $2\sqrt{(LA/\pi)}$ and $2\sqrt{(\pi LA)}$,
212 respectively, where *LA* is the luminal area, so that comparisons could be main to
213 manual measurements. The square root of the wall area, $\sqrt{WA}$, was calculated by
214 $\sqrt{(\pi * (BWT^2 + LD * BWT)}$. Approximately 200 image slices were analyzed for each
215 animal at one airway per apical lobe between the 4^{th} and 6^{th} generation. The $\sqrt{WA}$ of all
216 image slices were plotted over the luminal perimeter for each animal, and a linear
217 regression line was retrieved. The $\sqrt{WA}$ at various luminal perimeters (e.g., Pi2 and Pi4)
218 were estimated on the regression line. Since the mean luminal perimeter with the

automated method approximated 4 mm, Pi4 was used as the primary analysis, and Pi2 was used as a sensitivity analysis. The segmentation of the airway lumen was conducted using ImageJ (NIH, Bethesda MD), and the other image processing and analysis were fully automated using a lab-made computer software package based on LabVIEW, version 17.0 (National Instrument, Austin TX).

Histopathologic analysis

Whole left lungs were inflated to a pressure of 25 cm of water and instilled by 70% alcoholic formalin for a minimum of 48 hours prior to sectioning and paraffin embedding. Tissues were HE stained and airway wall thickness was determined from RGB color images of HE stained sections using Image Pro Plus 7 image analysis software (Media Cybernatics). Images were made with 4x, 10x, 20x, or 40x objectives and were obtained from each airway sectioned at approximately perpendicularly in the sections provided. For each airway, epithelial type (cuboidal or ciliated respiratory), and presence or absence of cartilage, mucus glands, and goblet cells were recorded (Supplemental Figure 4A). Using image editing software, images were prepared for analysis by erasing the area external to the wall so as to leave airway adventitia, cartilage, mucus glands, and smooth muscle. Material in the lumen was erased and the lumen filled with solid red (Supplemental Figure 4B). To measure the total area of the airway, the image was gray scaled and thresholded so as to form a representative black object (Supplemental Figure 4C), and the total area exported in μm^2 to an Excel spreadsheet data template. The software was appropriately calibrated for each objective magnification. The software was configured not to fill holes or spaces, as the

majority of apparently empty space is due to shrinkage during fixation and processing and is thus not present in life. The area of the lumen was determined by selecting the red object representing the lumen, then gray scaling, thresholding, and exporting the area in μm^2 for analysis. The perimeter of the luminal object was also collected and exported (Supplemental Figure 4D). From these raw data, we calculated estimated wall thickness as (total area – lumen area)/lumen perimeter; estimated airway luminal diameter as lumen perimeter/π, and the ratio of wall thickness/luminal diameter. Use of the perimeter of the luminal object estimates the luminal diameter, and thus wall thickness, of the airway at full diameter, without mucosal folding, which provides better estimates of size and wall thickness in life than circumference of a circle of the area of the luminal object. The data from the airways for each animal were collected individually. Ten to 25 airways (average 16.75) were analyzed per ferret.

Statistical analysis

Descriptive analysis was conducted with Graphpad Prism V7 (LaJolla, CA), and inferential statistics were conducted by Student's t-test or ANOVA with Tukey's post-hoc evaluation, as appropriate. Results are presented as means ± SD, unless indicated otherwise. $P<0.05$ was considered statistically significant. Regression analysis was conducted using SPSS V19 (IBM). Univariate regression was used to determine factors related to determinants of airway morphology, including smoking status, sex, and anatomic location (apical, medial, or caudal, as categorical variables), and laterality. Subsequently, multivariate backwards regression was used to assess the independent contributors to airway morphology.

Results

Bronchial Wall Thickness and Luminal Diameter

Bronchial wall thickness is an important marker of airway wall injury and is associated with chronic bronchitis in patients (7, 12, 14, 23). As depicted in representative images, after six months of cigarette smoke exposure, smoke exposed ferrets demonstrated greater bronchial wall thickness as compared to air controls (Figure 1B). Manual evaluation of BWT revealed cigarette smoke exposed ferrets had elevated mean BWT by 34% (0.58 ± 0.09 mm, n=23 vs. 0.43 ± 0.06 mm, n=19 control; $P<0.001$), (Figure 1C). Since BWT was partially dependent on airway size, we also examined luminal diameter (LD) and BWT/LD ratio. LD was 15% larger in smoke exposed ferrets measured at the same anatomic locations (0.73 ± 0.11 mm smoke vs. 0.63 ± 0.11 mm air controls; P=0.003; Figure 1D), which may be an early indicator of altered airway tone, or alternatively airway dilatation induced by chronic bronchitis. Despite these changes, mean BWT/LD was 16% higher in smoke exposed ferrets (0.82 ± 0.15 mm smoke exposed vs. 0.71 ± 0.13 mm controls; P=0.013) (Figure 1E), indicating BWT is induced by smoking, even when controlled for changes in airway size.

To compare with μCT, we conducted histopathological analysis of airway wall thickness by morphometry, capturing the distance from the surface of the epithelial cells to the surrounding smooth muscle, but not overlying mucus since histopathological fixation disrupts mucus continuity with the epithelium (see Figure 1B inset), by a veterinary pathologist familiar with the ferret lung and blinded to exposure assignment. Results in airways from 0.53 to 0.93 mm luminal diameter (chosen to reflect

approximate size of airways measured by μCT) indicated smoke exposed ferrets had no increase in airway wall thickness compared to air control ferrets (0.35 ± 0.03 mm smoke exposed vs. 0.52 ± 0.16 mm controls; P=0.067), indicating the principle reason for increased BWT by μCT was likely due to mucosal thickening.

Regional Differences in Airway Wall Thickness

Having established that smoke exposed airways exhibited significantly greater bronchial wall thickening as compared to air control exposed ferrets, we next sought to determine whether particular lobes were more affected, as seen in human COPD patients (18, 24). Likely related to differences in airflow in ferrets that alter deposition of cigarette smoke constituents, increased BWT performed by manual measurement disproportionately affected the caudal (40% increase, $p<0.001$) and apical lobes (37% increase, $p=0.001$) of ferrets exposed to cigarette smoke as compared to controls, whereas the medial lobe (25% increase, $p=0.005$) was less severely affected by smoking (Figure 2A). The effect of smoking on airway caliber varied substantially by anatomic location; the apical lobe of smoke exposed ferrets exhibited increased diameter (by 23%), whereas the medial (8%) and caudal (19%) lobes were less dilated (Figure 2B). Consequently, ratiometric BWT/LDs measurements were also increased by smoking when all airways were considered (Figure 2C), and were relatively consistent by anatomic location (13%, 17%, and 19% increased by smoke exposure over air controls at the apical, medial, and caudal lobe, respectively); considered individually, the changes in BWT/LD at each individual anatomic location were not statistically significant, but were as a group (Supplemental Table 2).

311

312

313 *Regression analysis*

314 As multiple different variables could be influencing airway dimensions, we next
315 performed regression analysis to account for potential factors independently, using
316 every airway measurement in the dataset. Univariate analysis for an effect on BWT
317 demonstrated smoke exposure (ß=0.148, indicating smoking had increased BWT 0.148
318 mm on average; $P < 0.001$) and apical anatomic location (ß=0.064, $P<0.001$) each had
319 significant contributions to bronchial thickness in ferrets, whereas laterality and sex had
320 no effect (Table 1A). Similar to BWT, BWT/LD ratio was also significantly affected by
321 smoke exposure (ß=0.080; $P = 0.003$) and anatomic location (ß=0.044; P=0.007).
322 Likewise, smoking (ß=0.099, $P<0.001$) and male sex were associated with increased
323 airway dilation. (ß= 0.119, $P<0.001$).

324 To account for each of these variables independently, we then conducted
325 multivariate backwards regression to determine dominant contributors to airway
326 morphology, starting with all variables noted in Table 1A. In the most parsimonious
327 model for determinants of BWT (R^2=0.368, $P<0.001$, N=252), smoke exposure and lung
328 region were each independent determinants of increased airway thickness (Table 1B).
329 For BWT/LD ratio (R^2=0.141, $P<0.001$, N=252), smoke exposure (ß=1.192; $P<0.001$),
330 female sex (ß=0.855; $P<0.001$), and anatomic location (ß=0.444; $P<0.005$) each
331 remained in the final model. Similarly, for LD (R^2=0.166, $P<0.001$), smoke exposure
332 (ß=0.093; $P<0.001$), anatomic location (ß=0.049; P=0.001), and male sex (ß=0.115;
333 $P<0.001$) were significant. In aggregate, these findings indicate smoke exposure has a

strong effect on BWT and BWT/LD, even when controlled for covariates that influence these parameters.

Airway Wall Thickness as measured by Pi2

Next we standardized measurements of airway abnormality in ferrets that closely modeled human airway disease detection using calculated airway wall thickness expressed as the square root of the wall area of a theoretical airway, as described in detail in the methods section; in the case of humans, this is a 10 mm internal perimeter airway (Pi10) as previously described (7, 12, 14, 19). For the ferret equivalent, first, we observed pronounced differences between smoke exposure groups indicating a consistent increase in wall area across various luminal perimeters (Figure 3A). The probability density function of the inner airway perimeter of control ferrets indicated 65% of the airways measured were between 1.5 and 2.5 mm, with a mean perimeter of 1.94 mm (Figure 3B); thus, we used calculation of $\sqrt{WA}$ of a theoretical 2 mm perimeter airway for each ferret (i.e. Pi2) to assess difference between groups. Regression analysis on an individual ferret basis was used to calculate the $\sqrt{WA}$ for the theoretical 2 mm perimeter airway (Figure 3C,D). Pi2 was 21.5% higher in smoke exposed ferrets as compared to air controls (1.458 ± 0.196 mm smoke exposed vs. 1.199 ± 0.151 mm controls; $P<0.001$, Figure 3E). These findings indicated Pi2 provided a strong indicator of the effects of smoking, with excellent discrimination between groups using a method that is translatable to human studies and incorporates those advantages.

Inter-analyst reproducibility

To assess the influence of analyzer on manual measurements, we trained a second analyzer on a representative dataset of 10 ferrets, and assessed reproducibility of mean airway wall measurements per ferret between operators after blinding to exposure assignment. While there were systematic differences in the measurement of BWT, LD and BWT/LD between analyzers, the relative difference in BWT (30.9% increase in smoke exposed ferrets vs. air controls by analyst #1 vs. 38% by analyst #2) and BWT/LD (19.4% vs. 41.7%) between smoke exposed ferrets as compared to air controls remained relatively consistent and detectable (Supplemental Figures 5A, B). Similar conclusions were true for inter-analyst differences in Pi2 measurements (Supplemental Figure 5C). Bland-Altman plot showed differences between analysts were not related to airway thickness and within 95% confidence of each other (Supplemental Figure 5D). This suggested that airway morphometry measurements were robust in terms of ability to distinguish disease phenotype, but also suggested that semi-automated measurement could be potentially advantageous to avoid analyst-dependent differences in absolute quantitation.

Semi-automated airway analysis

To address the between-operator differences in airway measurements, increase the number of measurements possible in a given dataset, and transition to actual measurement vs. a calculated assessment of airway wall area, important in the case of asymmetry, we developed a semi-automated airway wall measurement algorithm, and applied this to the upper airways. Figure 4A illustrates the process for semi-automatic BWT measurement. The individual BWT measurements (N=200 axial slices per ferret x

23 smoke, 19 control) was elevated in smoke exposed ferrets (0.590 ± 0.077 mm) as compared to that of the air control group (0.561 ± 0.074 mm; P<0.0001; Figure 4B). As compared to manual measurements in the same ferrets, semi-automated measures of bronchial wall thickness were larger, reflecting the algorithm calculated the thickness of airways more proximal than could reliably be obtained evaluating a single axial slice, but continued to distinguish BWT in smoke exposed ferrets vs. air controls (Supplemental Figure 6).

To conduct Pi measurements with the semi-automated methods, we conducted a similar analysis procedure as performed with manual measurements, but used a larger Pi to reflect the fact that more proximal airways were captured. The probability density function (PDF) of luminal perimeter in the control group indicated forty percent of the airways measured were between 3.5 and 4.5 mm, with a mean perimeter of 4.293 mm thus, we used calculation of √WA of a theoretical 4 mm perimeter airway for each ferret (i.e. Pi4) to assess difference between groups (Figure 4C). Figure 4D shows a scatter plot of measured $\sqrt{WA}$ vs. luminal perimeter of a representative animal in each group together with a linear regression line, suggesting the relationship is linear in each case (P<0.001 for each). Figures 4E and 4F show the $\sqrt{WA}$ vs. luminal perimeter regression lines of each animal in the control (n=19) and smoke groups (n=23), respectively, each constructed from ~200 data points. The mean $\sqrt{WA}$ for a 4 mm luminal perimeter airway is indicated with a horizontal dotted line. The Pi4 of animals in the smoke exposed group was 1.874 ± 0.110 mm, significantly larger than that in the control group (1.795 ± 0.090 mm; p=0.015; Figure 4G). As a sensitivity analysis and to compare with Pi estimates conducted with the manual measurements, the Pi2 in the smoke group also

403 was higher than that in the control group, approaching statistical significance (1.622 ±
404 0.111 mm *vs.* 1.533 ± 0.184 mm; p=0.061). Overall, these results confirmed findings
405 with manual airway measurements in a fashion that was more robust and that could be
406 applied to a greater number of representative airways.
407
408 *Longitudinal Changes in Airway Dimensions with Smoke Exposure*
409 To assess airway thickness evolves over time in smoke exposed ferrets with
410 chronic bronchitis, we next performed quantitative μCT analysis at baseline and monthly
411 thereafter through six months in a sub-cohort of smoke exposed ferrets (N=3). As seen
412 in Figure 5A, mean BWT by manual measurement method steadily increased over time,
413 with initial changes detectable as early as two months of cigarette smoke exposure
414 (24% increase, $P<0.05$) that plateaued by 4 months (48.8% increase). Semi-automated
415 measurements showed BWT steadily increased with cigarette smoke exposure, and
416 became statistically significant at five months (Figure 5B, 10% increase, P=0.016).
417 Similarly, automated Pi4 measurements also increased over time (Figure 5C),
418 becoming statistically significant ($P<0.05$) at 3 months and peaking with a 7.7%
419 increase (5 months, P=0.006). In contrast to smoke exposure, air control ferrets did not
420 increase BWT over time, either by manual (Figure 5D) or semi-automated
421 measurements (Figure 5E). These results showed cigarette smoke exposure induces
422 airway disease as detected by several complimentary measures of airway wall
423 abnormalities readily detected by μCT, and is first evident by 2-3 months of exposure.
424

Discussion

Here we have demonstrated a technique to study structural airway changes using high-resolution μCT in a ferret model of smoking induced chronic bronchitis, a technique highly sensitive to airway disease in humans with COPD (7, 12, 14, 19). This was successfully implemented by the manual measurement of 6 segmental airways, similar to a human study that established the correlation of bronchial wall thickness with airway reactivity (19), and also by semi-automated data extraction that improved the number of airways assessed, the range of airways measured, and the throughput and potential bias of the assessments. Both between analyst reproducibility and the use of semi-automated version of the method demonstrated complementary findings that were also reproducible, providing definitive conclusions. We further showed that cigarette smoke exposure in ferrets caused an increase in bronchial wall thickness that progressed over the course of a longitudinal six month study as compared to air control ferrets, expanding our prior understanding of airway disease in the model (20) and firmly establishing causality. As compared to histopathological analysis that did not show that smoke exposure increased airway wall thickness, but did not capture the overlying mucus layer, our results suggest that mucus accumulation may be the dominant factor underlying the difference in μCT parameters, although other aspects including differences related to in vivo measurements for CT imaging vs. ex vivo measurements for histology, or technical issues related to tissue processing and variable washout of mucus could also have contributed to this discrepancy. Of note, this is consistent with our prior report where global changes in epithelial thickness were not observed, even though epithelial cell height was increased (20).

449 The segmental and sub-segmental airway wall thickness is commonly measured
450 using Pi10 in human subjects, and has proved to be a superior biomarker of airway
451 disease than other CT-based metrics (7, 12, 14, 19). Several studies demonstrated the
452 significance of Pi10 measurements towards estimating airway narrowing associated
453 with COPD (7, 12, 14, 19), and Pi10 has major advantages for sensitively detecting
454 disease while avoiding bias in the estimate of between-subject differences in airway
455 sizes. As an additional method developed in our study, in an effort to recapitulate the
456 measurement of bronchial wall area in humans to estimate airway size for a
457 standardized airway caliber on an individual basis (7, 12, 14, 19), we successfully
458 implemented theoretical airway caliber calculations for the square root of bronchial wall
459 area for the six medium sized airways we calculated manually, and also the ~200 semi-
460 automated measurements of BWA we measured directly in each ferret. Both the
461 manual measure of bronchial wall area for theoretical airways on an individualized ferret
462 basis (Pi2), and the semi-automated version (Pi4) demonstrated similar findings, in that
463 they each indicated a 5-20% increase in smoke exposed ferrets as compared to air
464 controls, and did so as soon as 2-4 months following initiation of smoke exposure.
465 These results provided a non-biased and potentially powerful approach to quantify
466 airway changes over time, and clearly demonstrated the deleterious effects of smoking
467 on airway morphometry that occur soon after first exposure, even though the intensity of
468 smoking was not massive. Noting that the semi-automated measure was based on
469 ~200 points to determine the regression line necessary to calculate theoretical airway
470 perimeter, as compared to many fewer points with manual measurements, we suspect
471 semi-automated Pi4 will be particularly valuable in future studies of pathophysiological

change or therapeutic response, noting that Pi4 did include airways with a larger airway circumference, and thus may also report on distinct pathophysiological processes occurring in medium-sized airways.

The protean effects of cigarette smoking on airway pathophysiology continue to emerge, and have been delayed in part by the challenges of modeling the disorder in humans (3). Development of the ferret model that exhibits chronic bronchitis in addition to emphysema, a unique pathophysiology as compared to rodents but that closely resembles human disease, provides an opportunity to better understand the human condition if appropriate endpoints can be developed and implemented, overcoming modest limitations posed by limited availability of ferret-specific protein reagents (20). In ferrets, the effects of the cigarette smoke were most pronounced in the caudal and apical regions of the lungs, areas most prone to particle deposition in the former (6) and consistent with central airway disease in humans in the case of the latter (21). More detailed analysis of how pathophysiology might differ by anatomic region provide an avenue for future research. Interestingly, the effects of sex were not prominent, except for differences in BWT/LD ratio, suggesting that despite their sexually dimorphic characteristics with respect to overall animal size, the effects of smoking were prominent in each. This sex-based difference in airway changes is also consistent with that seen in human airways (11, 13). While we focused on airway disease, there may be other radiographic findings warranting attention in future work, including radiographic estimates of emphysema or the characterization of patchy alveolar opacities that are transient in nature.

494 A potential limitation of our study is that the resolution of the μCT scans do not
495 yet fulfil the full capability of the instrumentation, principally due to limitations imposed
496 by motion artifacts (i.e. beaming) associated with imaging a breathing animal, despite
497 use of respiratory gating. This was noted as smaller voxel reconstitution did not
498 improve end-resolution. The limit for reliability in airway wall measurements will be
499 primarily determined by the spatial resolution of image. With current methods, the
500 spatial resolution is approximately 0.12 mm; further improvements would necessitate
501 longer imaging times and subsequently computational power for image processing.
502 Improved gating procedures, or institution of breath hold maneuvers to pause breathing
503 during image acquisition, could also be developed to improve limits of resolution,
504 allowing sufficient resolution to ultimately address new questions such as the severity of
505 emphysema regional differences in disease expression, or the occurrence of airway
506 drop out detectable in human specimen by frozen tissue analysis and ultra-high
507 resolution procedures (9, 10, 15, 16). While manual measurements were limited by
508 throughput and the ability to measure the exact same location over time, semi-
509 automated measurements we were able to increase the number of measures and allow
510 for improved estimates of Pi4 that proved sensitive to disease as it emerged. However,
511 our semi-automated method for bronchial wall thickness measurements were developed
512 under the assumption that the airway is relatively straight at that location. Thus, this
513 method may be suboptimal for curved airways.
514 In summary, we successfully developed μCT based metrics of airway disease in
515 a COPD ferret model, allowing within and between subject comparisons in vivo,
516 enabling longitudinal studies as pathology evolves. Results in comparison to

517 pathological interpretation demonstrated airway disease is principally due to changes in
518 the airway mucosa, as opposed to structural changes in the smooth muscle, and is
519 clearly induced by cigarette smoking in the model. We further show these metrics are
520 dynamic, and that quantification of airway thickening can readily be performed on an
521 individual ferret basis, providing a viable in vivo biomarker that can be exploited in future
522 studies. This sets the stage for use of airway wall parameters as a sensitive metric for
523 understanding biology that also has the potential for measuring the effects of novel
524 interventions affecting airway mucus or epithelial function.
525

526 **Acknowledgments**

527 The authors acknowledge institutional support through the University of Alabama Health
528 Services Foundation Institutional Endowment to purchase the μCT instrument.

529

Figure legends:

Figure 1. Structural analysis of smoke exposed ferret airways using µCT. (A) Representative image of ferret lung µCT scan. Red arrows show the locations where airway measurements were taken. **(B)** Representative coronal and axial projections of air control (upper panels) and 6 month smoke-exposed (lower panels) ferrets. Lower insets are magnified views of a representative airway selected for measurements. Yellow line indicates airway luminal diameter and red line represents BWT. Upper insets demonstrate the same measurements by histopathological analysis for comparison. **(C)** Manual BWT of smoke exposed and air control ferrets. Each point represents mean BWT of a single ferret derived from 6 airway measurements per ferret and N=42 ferrets (23 smoke, 19 control). ****P<0.0001 **(D)** Manual Mean luminal diameter. **P<0.01. **(E)** Manual Mean BWT/Luminal Diameter ratio. *P<0.05. Inferential comparisons by Student's t-test.

Figure 2. Anatomic location specific structural analysis of smoke exposed ferret airways using µCT. (A) Manual BWT of air control and smoke exposed ferrets by anatomic location. **(B)** Manual Luminal diameter. **(C)** Manual BWT/luminal diameter ratio. *P<0.05, **P<0.01, ***P<0.001. ****P<0.0001. Each region had two measurements per ferret (i.e. left, right) that were averaged to a single point estimate per ferret (N=23 smoke, 19 control). A single point estimate for each of three regions was included for each ferret in the all-region analysis (N=69 smoke, 57 control). Inferential comparisons by ANOVA with Tukey's post-hoc test.

Figure 3. Differences in calculated bronchial wall area for theoretical airways in ferrets. (A) Manual √WA vs. luminal perimeter plotted for each individual ferret airway (6 airways/ferret N= 23 smoke, 19 control), by smoke exposure status. Y-intercept (√WA) of the regression line was significantly greater in smoke exposed ferrets as compared to air control. ****P<0.0001 by linear regression slope comparison. **(B)** Manual Probability density function of airway luminal perimeter sizes of air control ferrets. **(C-D)** Manual Regression lines for each air control (C) and smoke exposed ferret (D). Dotted lines show mean √WA for 2 mm perimeter airways. **(E)** Manual Calculated √WA of the theoretical 2 mm perimeter airway (Pi2) from ferrets exposed to cigarette smoke vs. airway control. ****P<0.0001 by Student's t-test.

Figure 4. Semi-automated analysis of airway wall anatomy in smoke exposed and air control ferrets. (A) Semi-Automated image processing for measurement of bronchial wall thickness is illustrated in three steps: First, the entire airway luminal region is segmented, and a target airway generation is specified as indicated with yellow lines. Second, the 3-dimensional CT image is re-oriented for the target airway region (lumen & wall) to be vertical to the image slices. A representative image slice is indicated with a dotted rectangle. Third, the bronchial wall boundary is automatically determined in each image slice. Typically, about 200 image slices were analyzed for each animal at one airway per apical lobe between the 4^{th} and 6^{th} generation. **(B)** Box plots of the Semi-Automated bronchial wall thickness (BWT) in the control and smoke groups. N=6648 airways; ****P<0.0001 by Student's t-test. Boxes denote the 25^{th}-75^{th} percentile and error bars represent the range. **(C)** Semi-Automated probability density function of the luminal perimeter, when the 4-6^{th} generations of the apical airway were analyzed in the control group. **(D)** Semi-Automated scatter plots of $\sqrt{WA}$ vs. airway luminal perimeter of a representative smoke exposed and air control ferret, each plotted with a linear regression line. ****P<0.0001. **(E, F)** Semi-Automated linear regression lines of $\sqrt{WA}$ vs. airway luminal perimeters of each ferret from the air control (E) and smoke exposed (F) group. Mean $\sqrt{WA}$ at 4 mm luminal perimeter is indicated with dotted lines in each panel. **(G)** Semi-Automated calculated √WA of the theoretical 4 mm perimeter airway (Pi4) for each ferret in the air control and smoke exposed groups. *P=0.012 by Student's t-test.

Figure 5. Longitudinal cigarette smoke exposure increases BWT and Pi4. (A) 6-month longitudinal study of mean BWT derived from all anatomic locations manually measured in a sub set of ferrets (n=3) followed over the course of smoking-induced COPD. *P<0.05, ***P<0.001, ****P<0.0001. **(B)** 6-month longitudinal study plotting mean BWT of all anatomic locations by Semi-Automated analysis. *P<0.05 **(C)** Calculated bronchial wall area of theoretical 4 mm perimeter airways in the same longitudinal cohort by Semi-Automated analysis. *P<0.05. Inferential comparisons by one-way ANOVA and Tukey's post-hoc test. **(D)** Mean BWT derived from all anatomic locations as a single value per ferret manually measured in an age-matched air control cohort of 9 ferrets (N=1-5 measures at each time point). **(E)** Semi-automated BMT of same as in *D*.

Table 1. Manual regression analysis of determinants of bronchial anatomy by CT. (A) Univariate regression analysis of determinants of bronchial wall thickness. All variables, including smoke status, sex, and anatomic location (apical vs. medial vs. caudal lung lobe), and laterality (left vs. right) were modeled for contribution in determining BWT. **(B)** Multivariate backwards regression model for significant

607 determinants of bronchial wall thickness in COPD ferrets. All variables, including smoke
608 status, sex, and anatomic location and laterality were considered in the original model.
609 N = 252, P < 0.0001, R^2=0.368.

610

Univariate Regression				
	Beta	**Std. Error**	**R square**	**P Value**
Smoking Status	0.148	0.016	0.241	<0.001
Anatomical Location	0.064	0.011	0.124	<0.001
Male Sex	0.025	0.019	0.007	0.184
Laterality	0.511	0.009	0	0.830
Multivariate Backward Regression				
Smoking Status	0.015	0.002	0.368	<0.001
Anatomical Location	0.006	0.001	0.368	<0.001

611

612

613

614

References

1. Dougherty. "An Introduction to Morphological Image Processing." ISBN 0-8194-0845-X (1992).

2. **Bodduluri S, Reinhardt JM, Hoffman EA, Newell JD, Jr., and Bhatt SP**. Recent Advances in Computed Tomography Imaging in Chronic Obstructive Pulmonary Disease. *Annals of the American Thoracic Society* 15: 281-289, 2018.

3. **Churg A, and Wright JL**. Animal models of cigarette smoke-induced chronic obstructive lung disease. *Contrib Microbiol* 14: 113-125, 2007.

4. **Fisher JT, Zhang Y, and Engelhardt JF**. Comparative biology of cystic fibrosis animal models. *Methods Mol Biol* 742: 311-334, 2011.

5. **Fricker M, Deane A, and Hansbro PM**. Animal models of chronic obstructive pulmonary disease. *Expert Opin Drug Discov* 9: 629-645, 2014.

6. **Ganguly K, Carlander U, Garessus ED, Friden M, Eriksson UG, Tehler U, and Johanson G**. Computational modeling of lung deposition of inhaled particles in chronic obstructive pulmonary disease (COPD) patients: identification of gaps in knowledge and data. *Crit Rev Toxicol* 1-14, 2019.

7. **Grydeland TB, Thorsen E, Dirksen A, Jensen R, Coxson HO, Pillai SG, Sharma S, Eide GE, Gulsvik A, and Bakke PS**. Quantitative CT measures of emphysema and airway wall thickness are related to D(L)CO. *Respir Med* 105: 343-351, 2011.

8. **Han MK, Agusti A, Calverley PM, Celli BR, Criner G, Curtis JL, Fabbri LM, Goldin JG, Jones PW, Macnee W, Make BJ, Rabe KF, Rennard SI, Sciurba FC, Silverman EK, Vestbo J, Washko GR, Wouters EF, and Martinez FJ**. Chronic obstructive pulmonary disease phenotypes: the future of COPD. *Am J Respir Crit Care Med* 182: 598-604, 2010.

9. **Hogg JC, Chu F, Utokaparch S, Woods R, Elliott WM, Buzatu L, Cherniack RM, Rogers RM, Sciurba FC, Coxson HO, and Pare PD**. The nature of small-airway obstruction in chronic obstructive pulmonary disease. *N Engl J Med* 350: 2645-2653, 2004.

10. **Hogg JC, McDonough JE, and Suzuki M**. Small airway obstruction in COPD: new insights based on micro-CT imaging and MRI imaging. *Chest* 143: 1436-1443, 2013.

11. **Kim V, Davey A, Comellas AP, Han MK, Washko G, Martinez CH, Lynch D, Lee JH, Silverman EK, Crapo JD, Make BJ, Criner GJ, and Investigators CO**. Clinical and computed tomographic predictors of chronic bronchitis in COPD: a cross sectional analysis of the COPDGene study. *Respir Res* 15: 52, 2014.

12. **Kim V, Desai P, Newell JD, Make BJ, Washko GR, Silverman EK, Crapo JD, Bhatt SP, Criner GJ, and Investigators CO**. Airway wall thickness is increased in COPD patients with bronchodilator responsiveness. *Respir Res* 15: 84, 2014.

13. **Kim YI, Schroeder J, Lynch D, Newell J, Make B, Friedlander A, Estepar RS, Hanania NA, Washko G, Murphy JR, Wilson C, Hokanson JE, Zach J, Butterfield K, Bowler RP, and Copdgene I**. Gender differences of airway dimensions in anatomically matched sites on CT in smokers. *COPD* 8: 285-292, 2011.

14. **Mair G, Maclay J, Miller JJ, McAllister D, Connell M, Murchison JT, and MacNee W**. Airway dimensions in COPD: relationships with clinical variables. *Respir Med* 104: 1683-1690, 2010.

15. **McDonough JE, Yuan R, Suzuki M, Seyednejad N, Elliott WM, Sanchez PG, Wright AC, Gefter WB, Litzky L, Coxson HO, Pare PD, Sin DD, Pierce RA, Woods JC, McWilliams AM, Mayo JR, Lam SC, Cooper JD, and Hogg JC**. Small-airway obstruction and emphysema in chronic obstructive pulmonary disease. *N Engl J Med* 365: 1567-1575, 2011.

16. **Muller NL, Staples CA, Miller RR, and Abboud RT**. "Density mask". An objective method to quantitate emphysema using computed tomography. *Chest* 94: 782-787, 1988.

17. **Ou C, Li Y, Wei J, Yen H-L, and Deng Q**. Numerical modeling of particle deposition in ferret airways: A comparison with humans. *Aerosol Science and Technology* 51: 477-487, 2017.

18. **Owsijewitsch M, Ley-Zaporozhan J, Kuhnigk JM, Kopp-Schneider A, Eberhardt R, Eichinger M, Heussel CP, Kauczor HU, and Ley S**. Quantitative Emphysema Distribution in Anatomic and Non-anatomic Lung Regions. *COPD* 12: 257-266, 2015.

19. **Patel BD, Coxson HO, Pillai SG, Agusti AG, Calverley PM, Donner CF, Make BJ, Muller NL, Rennard SI, Vestbo J, Wouters EF, Hiorns MP, Nakano Y, Camp PG, Nasute Fauerbach PV, Screaton NJ, Campbell EJ, Anderson WH, Pare PD, Levy RD, Lake SL, Silverman EK, Lomas DA, and International CGN**. Airway wall thickening and emphysema show independent familial aggregation in chronic obstructive pulmonary disease. *Am J Respir Crit Care Med* 178: 500-505, 2008.

20. **Raju SV, Kim H, Byzek SA, Tang LP, Trombley JE, Jackson P, Rasmussen L, Wells JM, Libby EF, Dohm E, Winter L, Samuel SL, Zinn KR, Blalock JE, Schoeb TR, Dransfield MT, and Rowe SM**. A ferret model of COPD-related chronic bronchitis. *JCI Insight* 1: e87536, 2016.

21. **Smith BM, Traboulsi H, Austin JHM, Manichaikul A, Hoffman EA, Bleecker ER, Cardoso WV, Cooper C, Couper DJ, Dashnaw SM, Guo J, Han MK, Hansel NN, Hughes EW, Jacobs DR, Kanner RE, Kaufman JD, Kleerup E, Lin C-L, Liu K, Lo Cascio CM, Martinez FJ, Nguyen JN, Prince MR, Rennard S, Rich SS, Simon L, Sun Y, Watson KE, Woodruff PG, Baglole CJ, and Barr RG**. Human airway branch variation and chronic obstructive pulmonary disease. *Proceedings of the National Academy of Sciences* 115: E974-E981, 2018.

22. **Tan O, Duan HL, and Lu WX**. [Review: Segmentation and classification methods of 3D medical images]. *Zhongguo Yi Liao Qi Xie Za Zhi* 26: 197-206, 2002.

23. **Teerapuncharoen K, Wells JM, Raju SV, Raraigh KS, Atalar M, Cutting GR, Rasmussen L, Nath PH, Bhatt SP, Solomon GM, Dransfield MT, and Rowe SM**. Acquired CFTR Dysfunction and Radiographic Bronchiectasis in Current and Former Smokers: A Cross-Sectional Study. *Annals of the American Thoracic Society* 2018.

24. **Tho NV, Trang le TH, Murakami Y, Ogawa E, Ryujin Y, Kanda R, Nakagawa H, Goto K, Fukunaga K, Higami Y, Seto R, Nagao T, Oguma T, Yamaguchi M, Lan le TT, and Nakano Y**. Airway wall area derived from 3-dimensional computed tomography analysis differs among lung lobes in male smokers. *PLoS One* 9: e98335, 2014.

25. **Vogelmeier CF, Criner GJ, Martinez FJ, Anzueto A, Barnes PJ, Bourbeau J, Celli BR, Chen R, Decramer M, Fabbri LM, Frith P, Halpin DM, Lopez Varela MV, Nishimura M, Roche N, Rodriguez-Roisin R, Sin DD, Singh D, Stockley R, Vestbo J, Wedzicha JA, and Agusti A**. Global Strategy for the Diagnosis, Management, and Prevention of Chronic Obstructive Lung Disease 2017 Report. GOLD Executive Summary. *Am J Respir Crit Care Med* 195: 557-582, 2017.

Figure 1

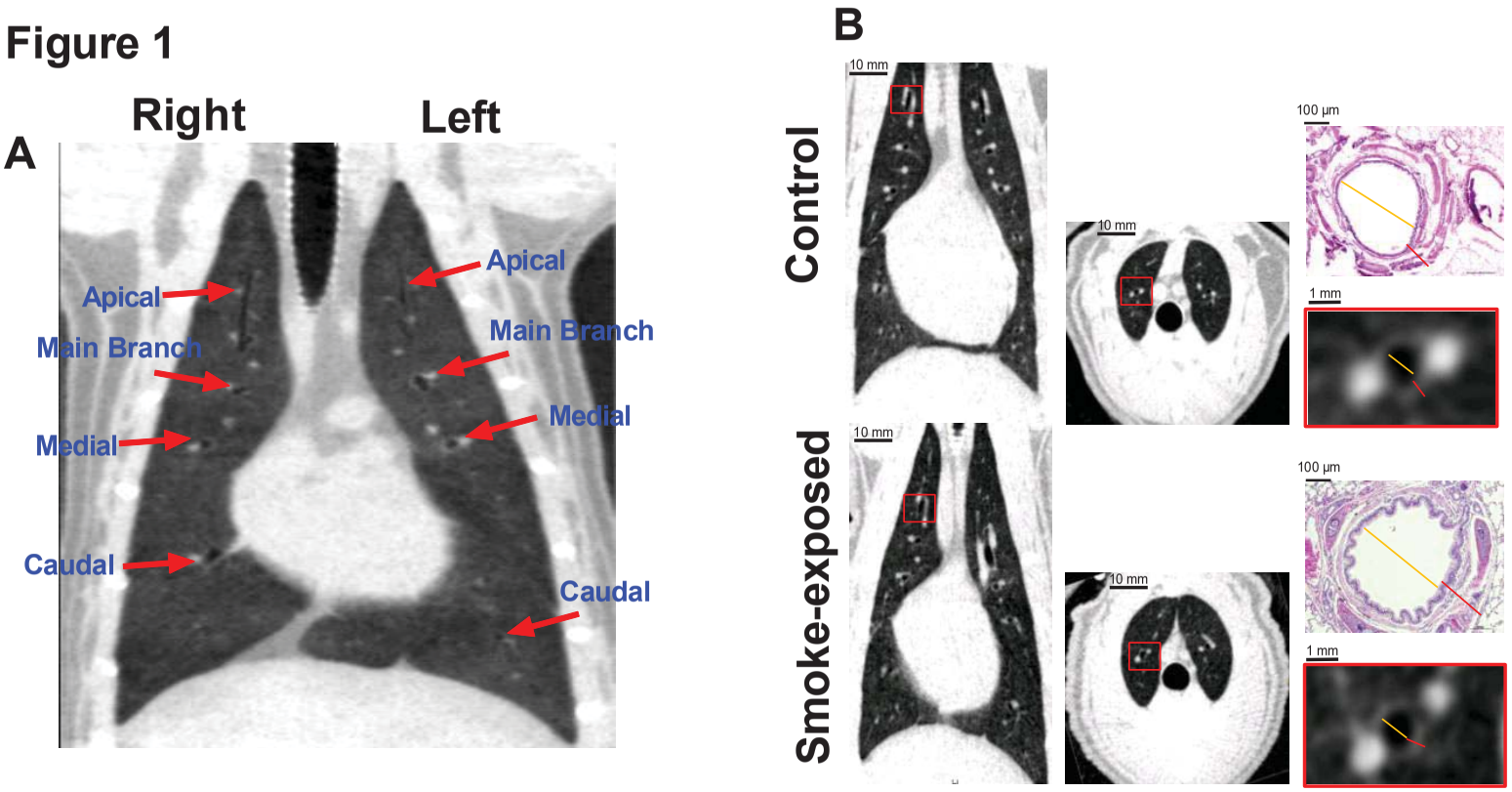

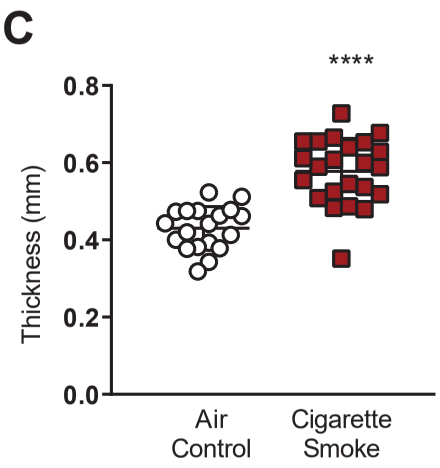

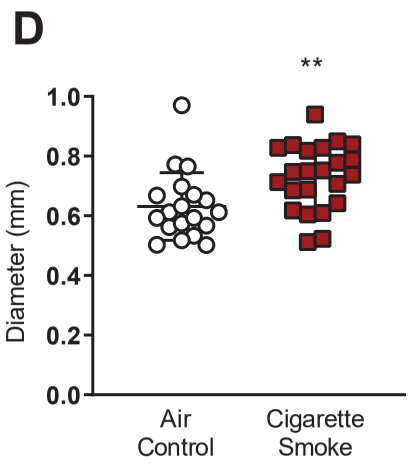

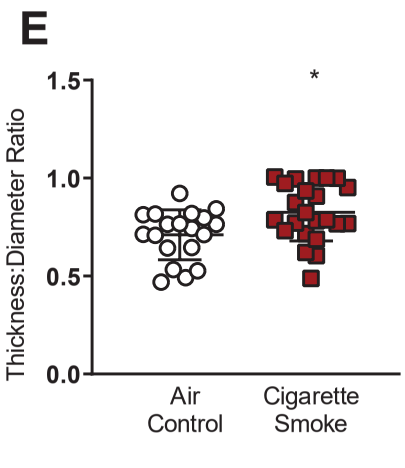

Figure 2

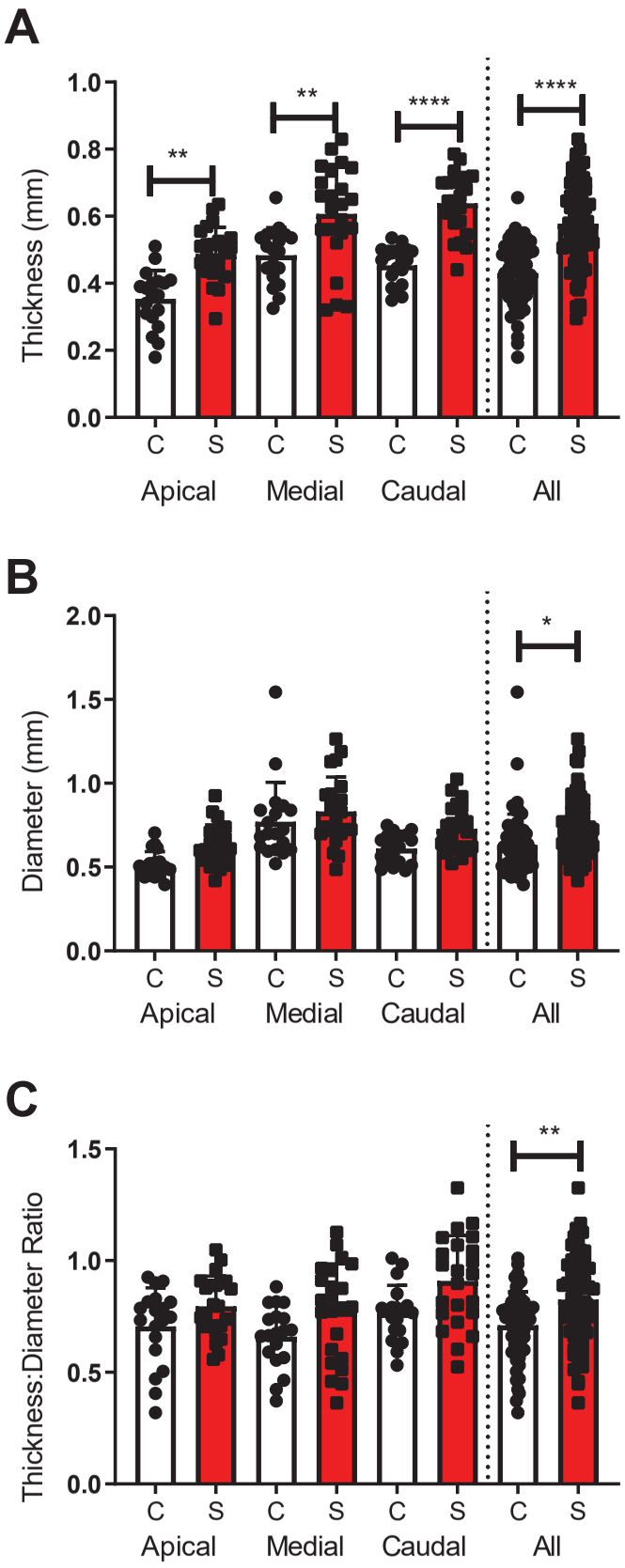

Figure 3

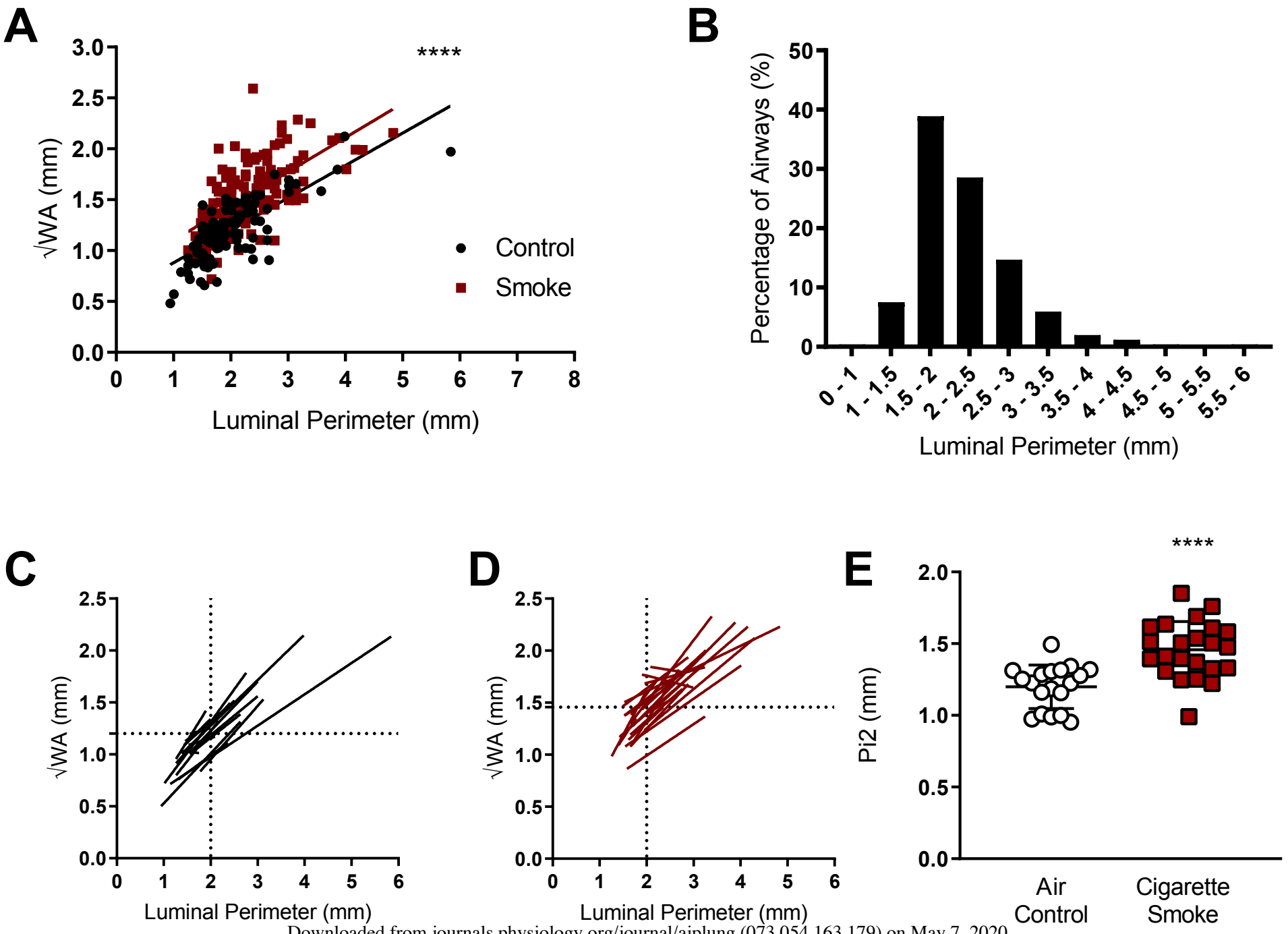

Figure 4

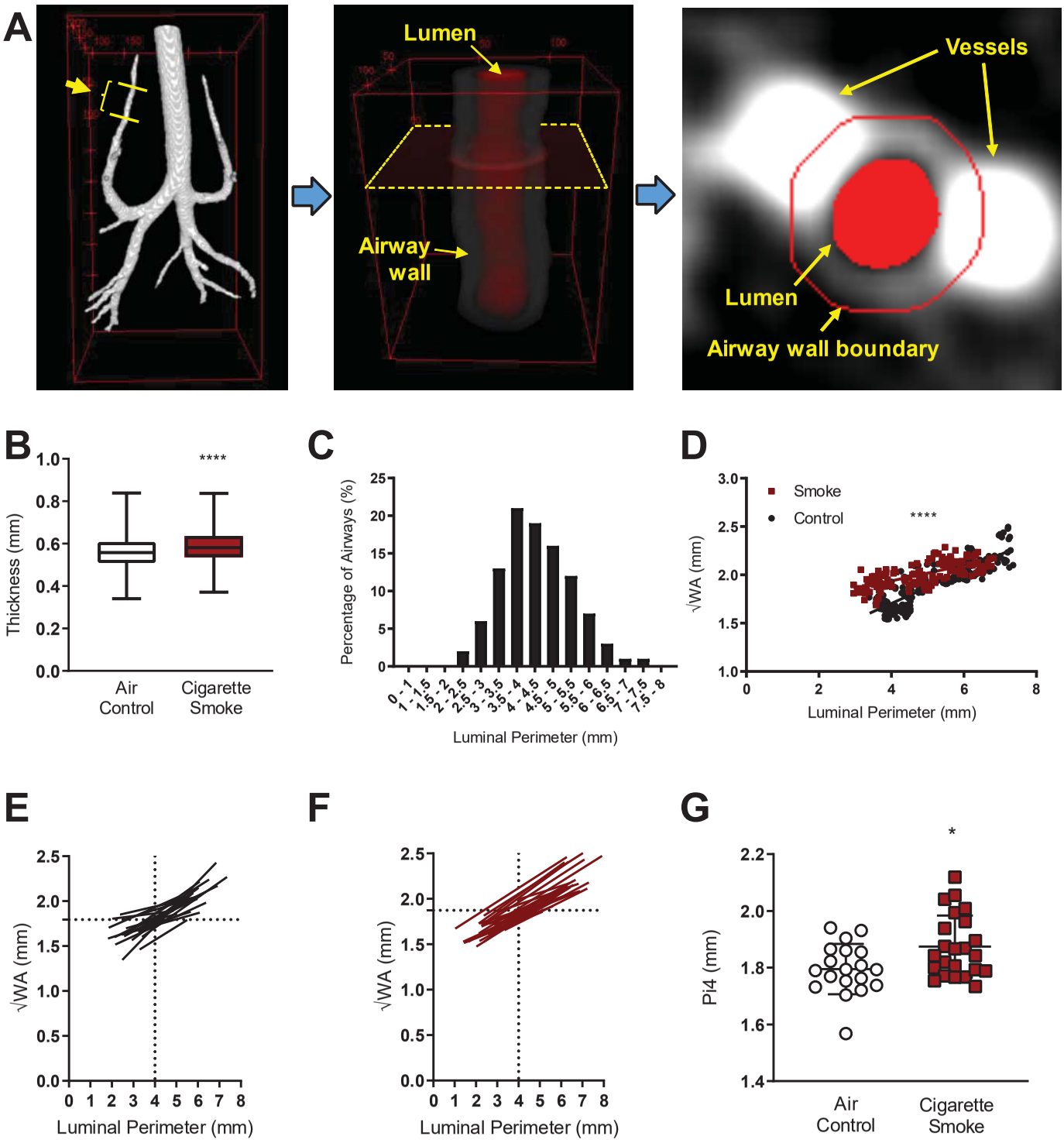

Figure 5